Paper 120, Bull. ISET. Vol. 9, No. 1, March 1972, pp. 23-36

DYNAMICS OF A FLEXIBLE STRIP FOOTING ON AN ELASTIC SOIL MEDIUM OF FINITE DEPTH*

BHASKAR NATH** AND PROVAKAR NATH***

INTRODUCTION

A Civil Engineer often encounters problems of flexible footings which carry dynamic loads. In order to evaluate the response of such footing-soil systems to arbitrary loads, the dynamic characteristics of the system must be determined accurately.

The general problem of such dynamical systems is very difficult and even approximate solutions to them are obtained (1) only after making simplifying assumptions. The following are recognised as the important characteristics of this class of problems:

(a) Coupling between the soil-medium and the footing:

Coupling occurs under both static and dynamic conditions of loading. The contact stresses deform the footing; these deformations, in turn modify the contact stresses. It will be seen later that the degree of coupling is represented by the stiffness of the soil medium, assumed to be elastic, relative to that of the footing.

(b) Conditions at the interface:

Under certain conditions of loading negative stresses may develop over some areas of the contact surface. However, as soil is usually assumed to be incapable of sustaining tensile stresses, this is not permitted and the problem now becomes a non-linear one.

(c) Energy dissipation in the system:

The mechanism of energy dissipation in the soil medium and its correct representation by a suitable numerical model is by far the most difficult aspect of the problem; in most real situations the phenomenon of radiation damping occurs in which stress waves carry away energy from the source of disturbance; numerical representation of this is difficult and at the moment a numerical solution of such problems can be attempted only by assuming the energy to be transported by plane waves (2, 3).

The above points illustrate the complexities of the problem and perhaps explain the absence of theoretical or experimental attempts to its solution. A number of analytical and experimental (6, 7) studies of the corresponding static problem are however available.

Present work primarily aims at determining the contact stress response under a flexible strip footing at a given frequency of motion and level of critical damping, when subjected to vertical harmonic loads. The assumptions made are, (1) no negative (i.e, tensile) stresses or separation is allowed to occur at the interface between the soil medium and the footing, so that the problem is a linear one and (2) loading on the footing is such that its deflections are symmetrical about the centre line, so that only symmetrical half of the geometry need be considered. The first assumption restricts the exciting frequencies to the sub-fundamental range, as negative stresses were found to occur at higher frequencies. The soil medium was assumed to be elastic, homogeneous and

---

* This paper was read at the Third Canadian Congress on Applied Mechanics, held in May 1971 at the University of Calgary, Alberta, Canada, and appears in abstract form in the proceedings of CANCAM 71.

** B.Tech., Ph.D., Lecturer in Civil Engineering, Queen Mary College, University of London, London.

*** B.Tech., M.Sc., Senior Scientific Officer, Road Research Laboratory, Crowthorne, England.

isotropic; its modulus of rigidity was taken as 2500 psi. and its Poisson's ratio as 0·30; the Young's modulus of the footing was taken as $2{\cdot}5\times10^6$ psi., while, the material of the footing was assumed to be 1·2 times denser than the soil. The problem was solved numerically by using the method of finite differences.

EQUATIONS OF MOTION

The geometry of the footing-soil system is shown in Fig. 1;-the footing is very long along the normal to the plane of the paper and carries harmonic vertical line-loads.

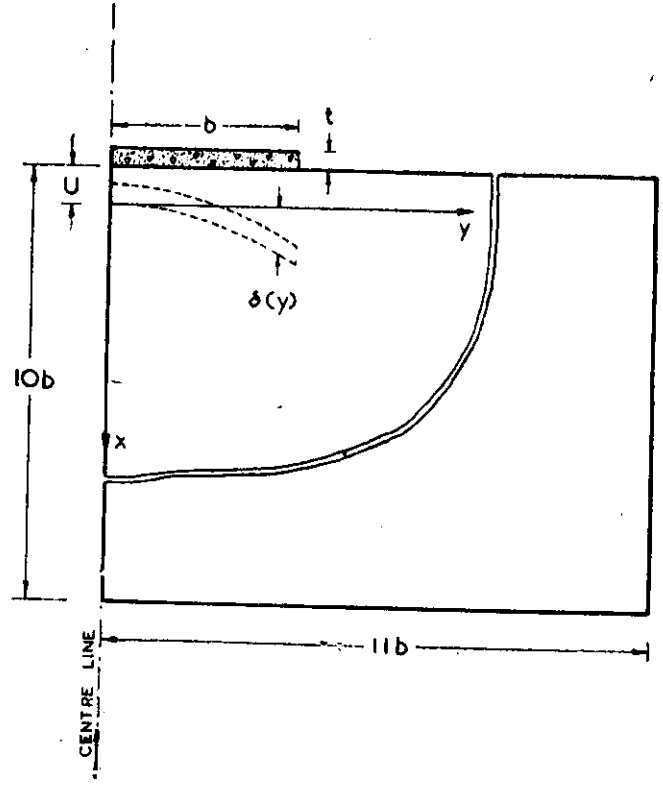

Fig. 1. Geometry of Footing-Soil System

The most obvious way to attempt a numerical solution to this plane-strain problem by using the method of finite differences would be to solve the following Lame's equations (8).

$$\alpha u_{,xx} + u_{,yy} + \beta v_{,xy} + \rho X = (1/c^2)\ddot{u} + (c'/G)\dot{u} \qquad \ldots(1a)$$

$$v_{,xx} + \alpha v_{,yy} + \beta u_{,xy} + \rho Y = (1/c^2)\ddot{v} + (c'/G)\dot{v} \qquad \ldots(1b)$$

where, u(x, y, t) and v(x, y, t) are components of elastic displacements in the soil in a Cartesian framework. (Note that all space-time variables and their derivatives are in general complex). Suffixes following the comma in Eqs. (1) denote differentiation with respect to space, while dots denote differentiation with respect to time; c′ and G are respectively parameters of equivalent viscous damping and modulus of rigidity of soil, while c is the velocity of shear waves in it; α and β are functions of the Poisson's ratio ν, given by

$$\alpha=(2-2\nu)/(1-2\nu) \quad \text{and} \quad \beta=1/(1-2\nu)$$

ρ is the mass density of soil and X and Y are components of body force accelerations. Solution of Eqs. 1 with appropriate initial and boundary conditions will give the elastic displacements and hence stresses within the soil.

There is one difficulty however in such a displacement-type analysis; convergence studies indicate that a small error in displacements (mainly u(x, y, t) in this case) obtained from Eqs. (1), produce a relatively large error in the computed stresses, particularly in areas of rapidly varying stresses. On the other hand, solution to the problem from strain equations gave very satisfactory results. The latter set of equations for this problem can be obtained (8) from Eqs. 1 by differentiation; it is not necessary to derive them here; we can simply write them in the compact matrix from as follows :

$$\begin{bmatrix} \alpha\frac{\partial^2}{\partial x^2}+\frac{\partial^2}{\partial y^2} & \beta\frac{\partial^2}{\partial x^2} & 0 \\ \beta\frac{\partial^2}{\partial y^2} & \alpha\frac{\partial^2}{\partial y^2}+\frac{\partial^2}{\partial x^2} & 0 \\ 2\beta\frac{\partial^2}{\partial x\partial y} & 2\beta\frac{\partial^2}{\partial x\partial y} & V^2 \end{bmatrix} \{e\}=\frac{1}{c^2}\ddot{\{e\}}+\frac{c'}{G}\dot{\{e\}} \qquad \ldots(2)$$

in which, $\{e\}=\{e_{xx}\ e_{yy}\ e_{xy}\}^T$ and V^2 is Laplace's operator in two dimensions.

The boundary conditions relevant to Eq. 2 are as follows :

$$e_{xy}=\sigma_{xx}\ (=\lambda\theta+2Ge_{xx})=0$$

at the free surface and far boundaries; the interface was assumed to be free of shearing stresses, so that,

$$e_{xy}=0 \text{ at } x=0 \text{ and } y=b.$$

Fig. 1 shows that the actual indentation of the footing into the soil is $\{U+\delta\}$; this indentation can now be incorporated into a boundary condition for e_{xx} at the interface; thus,

$$U(t)+\delta(y, t)=\int_H^0 e_{xx}\,dx \quad \text{at } x=0 \quad \text{and} \quad y=b \qquad \ldots(3)$$

Note that U(t) represents the indentation of the footing, assumed to be rigid, into the soil medium whose depth is H.

The other direct stress σ_{yy} was also assumed to vanish at the far boundaries; the problem however is not yet uniquely defined as no condition can be imposed on σ_{yy} at the free surface and at the interface. An indirect method given in Appendix I, was used to determine these boundary values of e_{yy}.

As for the footing, its equation of motion can be written as,

$$[S]\{\delta\}+[M]\ddot{\{\delta\}}+[T]\{e\}=\{f\} \qquad \ldots(4)$$

in which [S] and [M] are respectively stiffness and mass matrices of the footing and the vector $\{f\}$ represents the intensity of external loading on the footing; [T] is a rectangular matrix which operates on $\{e\}$ to give the direct stress vector $\left\{\sigma^1_{xx}\right\}$ at the interface; (note that in Eq. (4) as well as in other matrix equations factors due to finite difference manipulations and material properties are assumed to be implicit within the matrices).

PROBLEM SOLUTION

Let the numerical version of the matrix on the left side of Eq. (2) be [A], into which all relevant boundary conditions, as well as frequency parameters of harmonic motion have been inserted, so that it now reads, on inversion,

$$\{e\} = [A^{-1}]\{U+\delta\} \quad \ldots(5)$$

Noting that by definition,

$$\{\alpha^1_{xx}\} = [T]\{e\} \quad \ldots(6)$$

Eq. (5) can now be written as,

$$\{\sigma^1_{xx}\} = [TA^{-1}]\{U\} + [TA^{-1}]\{\delta\} \quad \ldots(7)$$

Also, as $\{\delta\}$ is null everywhere except at the interface, we may regard it as a vector for the interfacial pivots only; further, with [D] as the interfacial submatrix of $[TA^{-1}]$, Eq. (7) can now be written as,

$$\{\sigma^1_{xx}\} = [TA^{-1}]\{U\} + [D]\{\delta\} \quad \ldots(8)$$

in which the ranges of [D] and $\{\delta\}$ are equal to the number of interfacial pivots. It is also noted that the first expression on the right side of Eq. (8) gives the 'rigid' stresses corresponding to a very stiff footing.

Assuming that the frequency parameters, as well as the mass matrix are implicit in [S], the deflections $\{\delta\}$ can now be obtained from Eqs. (4) and (6) as,

$$\{\delta\} = [S^{-1}]\{f - \sigma^1_{xx}\} \quad \ldots(9)$$

Equations (8) and (9) illustrate the coupled nature of the problem, in which coupling occurs between the flexible footing and the soil. On eliminating $\{\delta\}$ and $\{\sigma^1_{xx}\}$ in turn from Eqs. (8) and (9), we can show that

$$\{\sigma^1_{xx}\} = [Z^{-1}TA^{-1}]\{U\} + [Z^{-1}DS^{-1}]\{f\} \quad \ldots(10)$$

and

$$\{\delta\} = -[\bar{Z}^{-1}S^{-1}TA^{-1}]\{U\} + [\bar{Z}^{-1}S^{-1}]\{f\} \quad \ldots(11)$$

in which $[Z] = [I+qDS^{-1}]$, $[\bar{Z}] = [I+qS^{-1}D]$, $q = Gb^3/Et^3$ and [I] = unit matrix.

It is noted that the factor q, which was so far implicit in the various matrices, represents the stiffness of the soil, relative to that of the footing; it also represents the degree of coupling between the soil and the footing, as will be seen later; as expected, with $q=0$, Eq. (10) gives the contact stresses under a rigid footing.

In order to determine the contact stresses due to an arbitrary line loading, Eqs. (10) and (11) must be solved with the auxiliary equilibrium equation,

$$\Sigma F + \{m\}^T\{\ddot{U}+\ddot{\delta}\} = \{W\}^T\{\sigma^1_{xx}\} \quad \ldots(12)$$

in which ΣF = total load on the footing and $\{m\}^T$ and $\{W\}^T$ are respectively its mass and weighting row matrices. They operate on $\{\ddot{U}+\ddot{\delta}\}$ and $\{\sigma^1_{xx}\}$ respectively to give inertial load and contact stress resultants.

The steps leading to the complete solution to the problem for a set of stiffness and dynamic parameters can be summarised as follows :

1. Set $\{\delta\}=\{0\}$ in Eq. (12) and eliminate $\{\sigma^1_{xx}\}$ between Eqs. (10) and (12) to give $\{U\}$.
2. Use this value of $\{U\}$ to determine $\{\delta\}$ from Eq. (11); substitute this value of $\{\delta\}$ in Eq. (12) and repeat the whole process.

The process is highly convergent and only a few cycles are required to get accurate estimates of $\{\delta\}$ and $\{U\}$. Eq. (5) can now be solved to give elastic strains (and hence stresses) everywhere within the domain of interest.

A simple fortran program was written to generate the matrices [A], [T] and [S] automatically, by using the finite difference methods. The domain was approximated by a total of 79 pivotal points, of which 5 represented the interface.

RESULTS AND DISCUSSION

First, it was necessary to determine the degree of accuracy of present results by comparing them with exact solutions. However, no exact solution to the dynamic case comparable with present geometry was available; Fig. 2 compares present static contact stresses under a rigid (q=0) footing with their exact (9) counterpart. The agreement is seen to be good, except around y=b, where it is poor. This is to be expected however, as there is a theoretical singularity of stresses at this point. Fortunately, this singularity was found to disappear for most loading conditions, when the footing was treated as flexible. Thus, results for the flexible footing are expected to be of a high degree of accuracy.

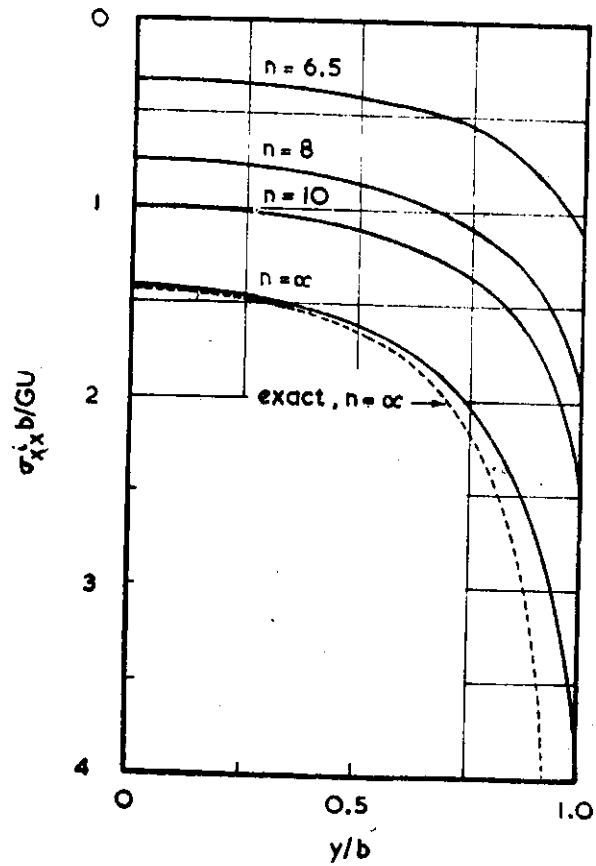

Fig. 2. Rigid Undamped Contact Stresses q=0; ν=0·3

It is also interesting to remark that static flexible stresses due to the present method were generally in good agreement with the experimental findings of reference 6; the small areas of disagreement that may be found in the distribution and magnitudes of contact

stresses between these two studies, can be attributed to the fact that the latter results were for a three dimensional soil medium.

Central line-load of P/length, $\nu = 0{\cdot}3$. $q = 0{\cdot}1$ and $0{\cdot}4$

Fig. 3 shows the undamped contact stress response at various sub-fundamental frequencies of motion, while, Figs. 4 and 5 show stress response at a relatively high critical damping of 20%; these plots clearly show that (a) at a given frequency and level of critical damping, the shape of the contact stress distribution curve depended entirely on

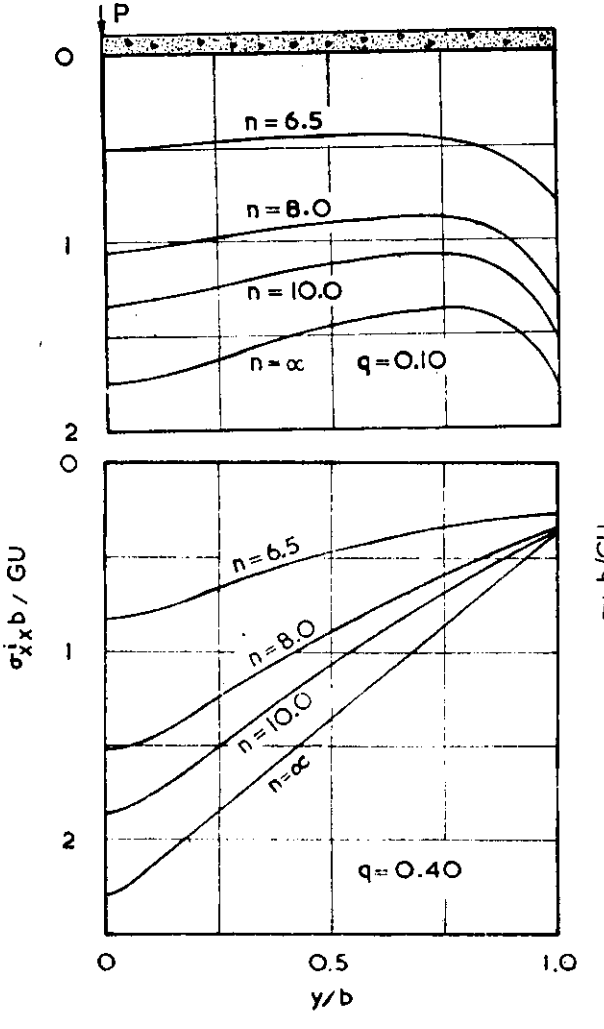

Fig. 3. Undamped contact stresses; $\nu = 0.3$

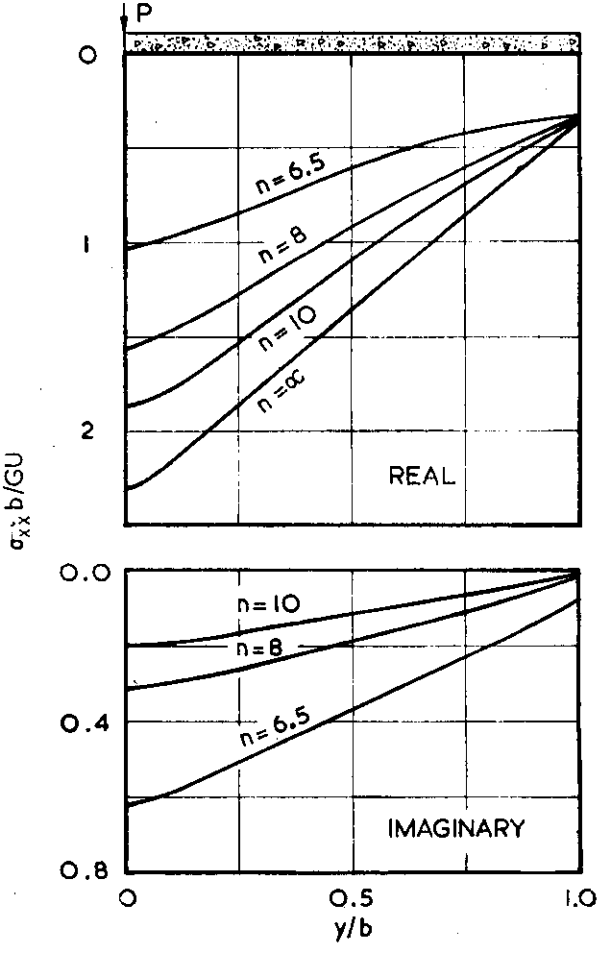

Fig. 4. Complex Contact stress Response
d = 0.2; $\nu = 0.3$; $q = 0.4$

the stiffness factor q, and (b) real response diminished with increasing frequency, while, as expected, response at quadrature with loading increased. Fig. 6 shows the undamped contact stress/penetration ratios, plotted along the interface at various exciting frequencies; these plots are found to be generally similar to the corresponding contact stress plots (Fig. 3); further, the data of Figs. 3 and 6 can be used, along with Eq. (12) to express contact stress response in terms of the central load P, if required.

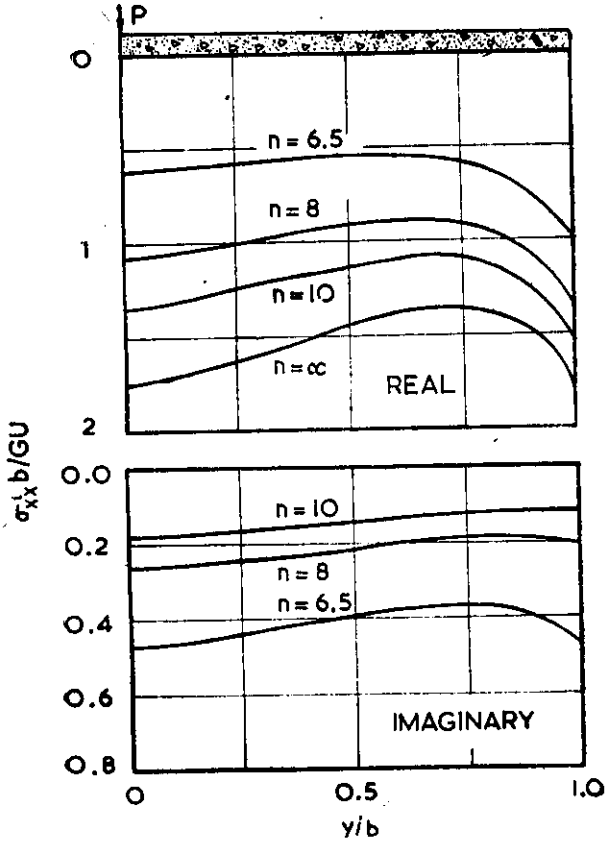

Fig. 5. Complex contact stress response
d=0.2; ν=0.3; q=0.1

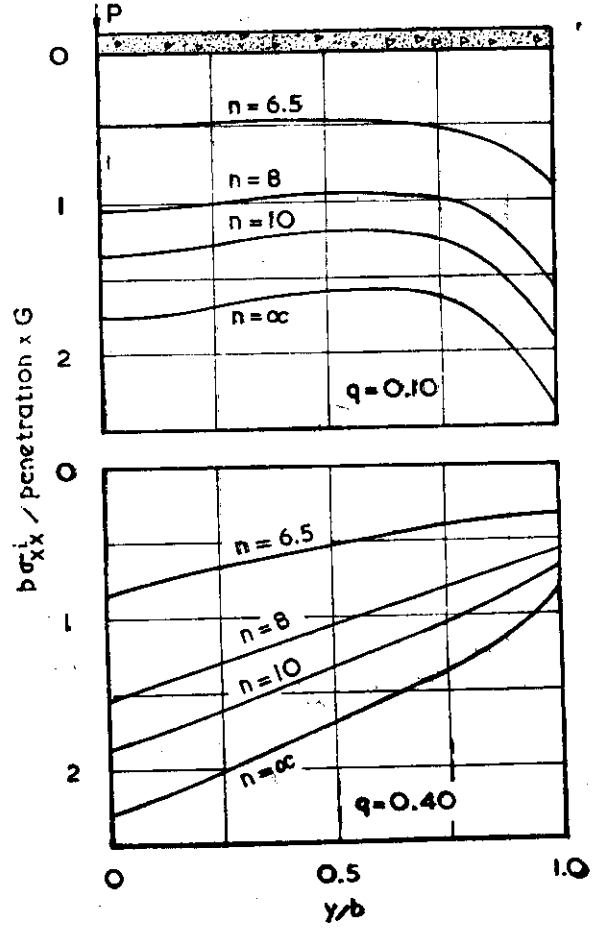

Fig. 6. Contact stress-penetration plots
d=0; ν=0.3

Line loads of 1000 lb/in at y=0 and 800 lb/in at y=±0·5b, ν=0·3 ; b=100 inches; q=0·1, 0·4 and 1·0 ; G=2500 psi; E/G=1000.

Figs. 7 and 9 show the undamped contact stress response at various stiffness factors. It is interesting to note that with increasing flexibility of the footing, the stress distribution curves became concave upwards; also, as before, response decreased with increasing frequency of motion and the contact stress/penetration plots (Figs. 8 and 9) were similar to the contact stress plots.

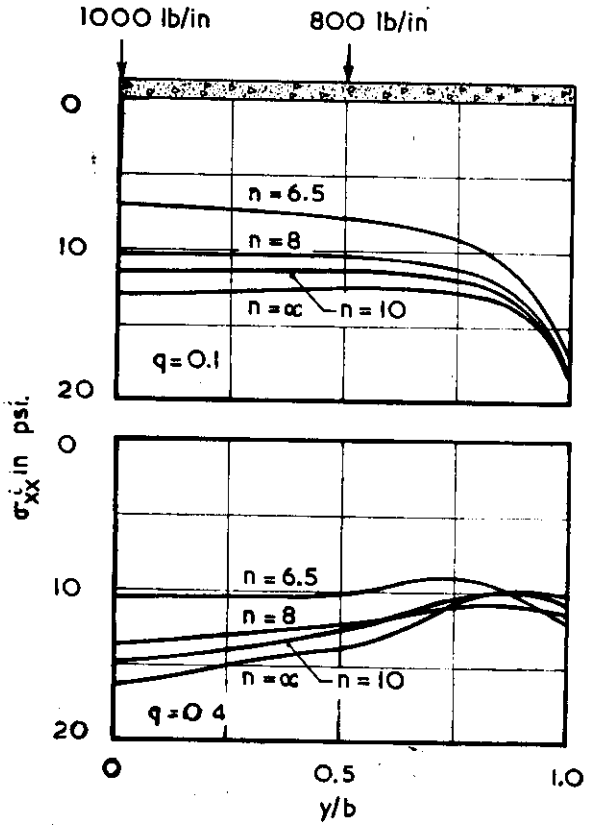

Fig. 7. **Response with multiple loads d=0; ν=0.3; b=100 in.; G=2500 psi.**

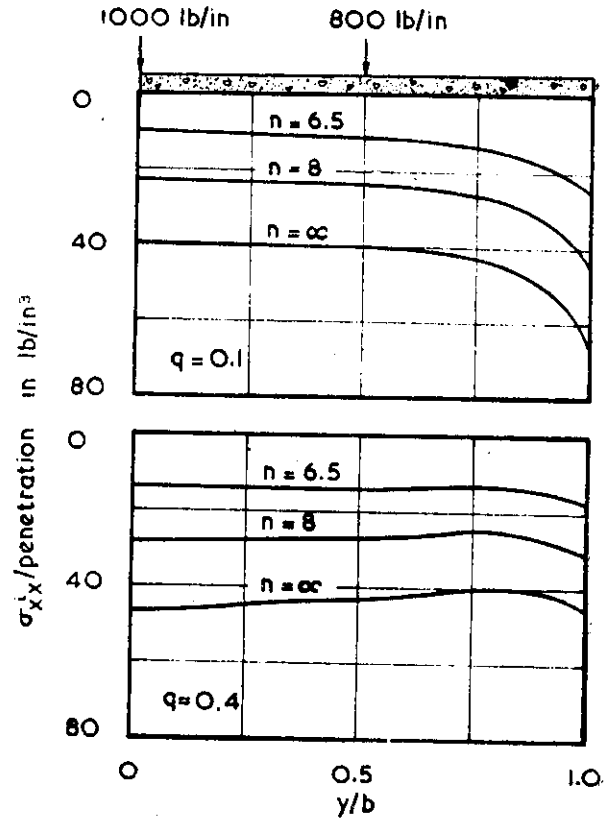

Fig. 8. **Contact stress penetration plots d=0; ν=0.3; b=100 in. G=2500 psi**

Line loads of 1000 lb/in at y=0 and 800 lb/in at y=±b; ν=0·3; b=100 inches; q=0·1, 0·4 and 1·0; G=2500 psi; E/G=1000;

Undamped contact stress response at various stiffness factors are shown in Figs. 10 and 12; here also the shape of the distribution curves were determined primarily by the stiffness factor q, and response decreased with increasing frequency of motion. Figs. 11 and 12 show the stress/penetration plots for the interface at various stiffness factors: here again, these plots are found to be similar to the contact stress diagrams.

The following observations are made on the results:

1. At a given frequency and level of damping, the distribution of contact stresses depended on the stiffness factor q; with a single central load, the distribution became concave upwards as the footing became increasingly flexible, with

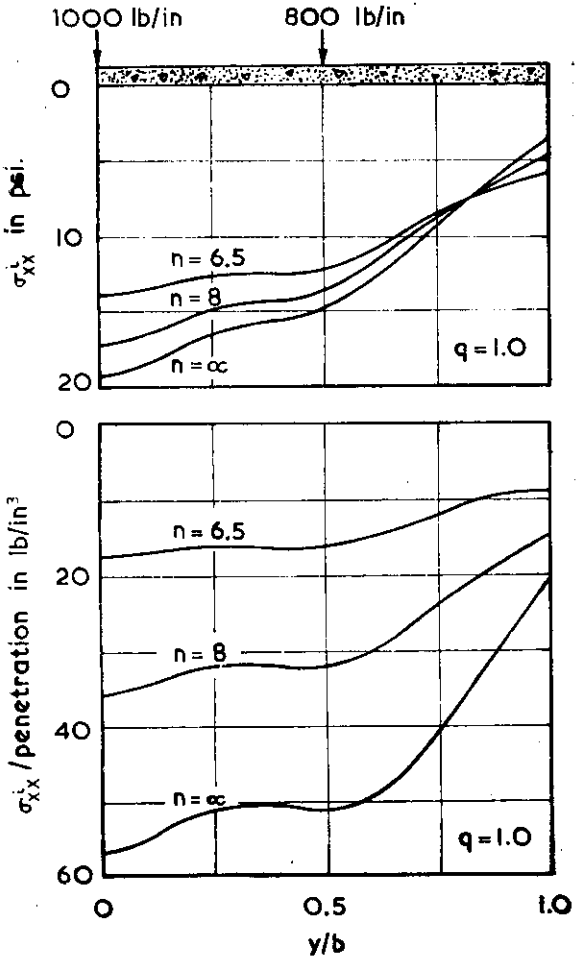

Fig. 9. Response with multiple loads
d = 0; $\nu = 0.3$; b = 100 in.;
G = 2500 psi.

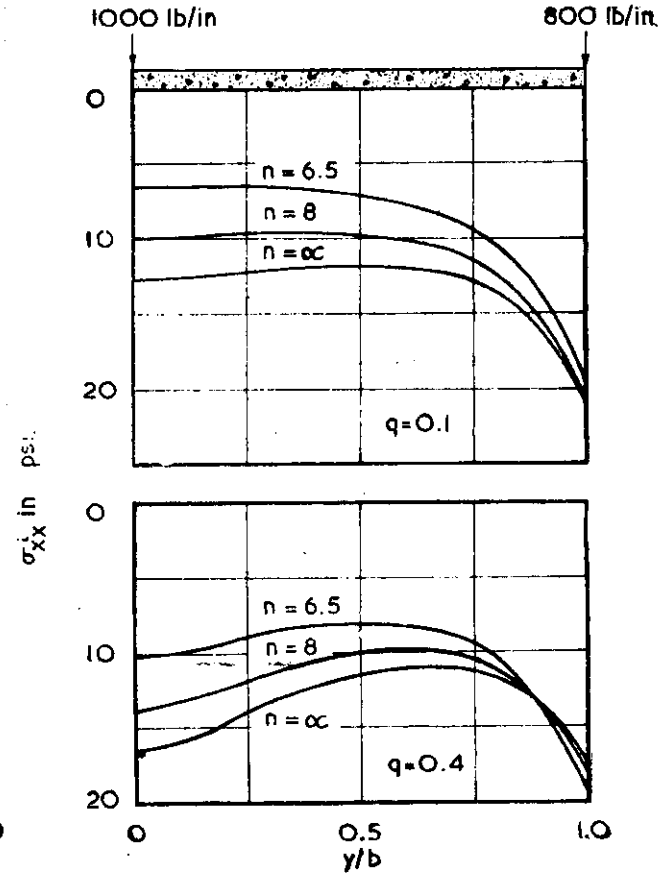

Fig. 10. Response with multiple loads
d = 0; $\nu = 0.3$; b = 100 in.;
G = 2500 psi

multiple loads and increasing flexibility on the other hand, the contact stresses depended increasingly on both location and magnitudes of the loads. For relatively stiff ($q < 0{\cdot}1$) footings, the distribution of contact stresses became insensitive to the magnitude and location of the loads and stress concentrations appeared at the edges. These observations generally agree with the findings of reference 6.

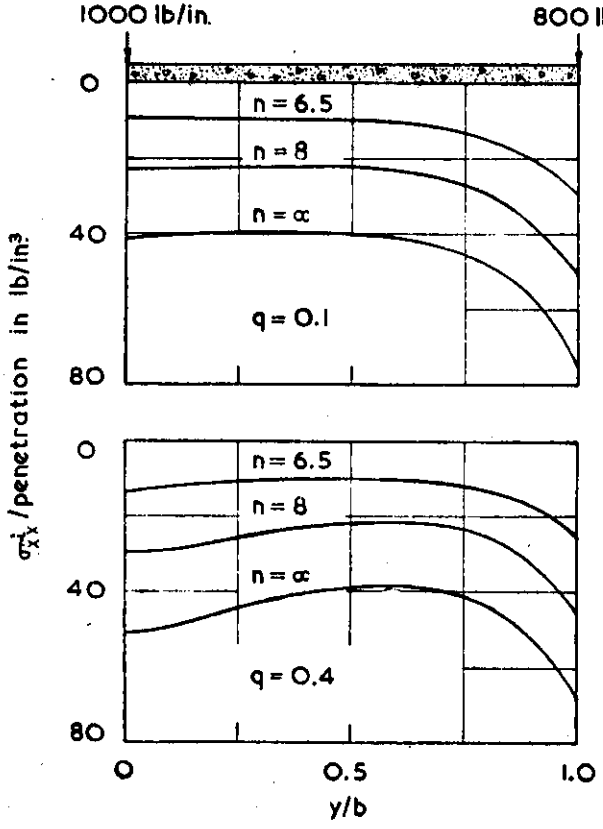

Fig. 11. Response with multiple loads. d=0; $\nu=0.3$; b=100 in.; G=2500 psi.

2. In all cases the stress response decreased with increasing frequency of motion. This indicates that the dynamic magnification factor (DMF) of stresses in the sub-fundamental range is less than unity, although, it will be high in the vicinity of the fundamental frequency of the footing-soil system. In a real situation however, damping (particularly radiation damping in infinite media) would severely attenuate DMF at high exciting frequencies; consequently, intolerably high values of DMF are not likely to occur and in any case would be confined to narrow frequency bands in the vicinity of the fundamental and low natural frequencies of the footing-soil system; under these circumstances; it seems likely that in a large variety of real systems, static stresses would represent the worst situation under harmonic conditions of loading.

3. The contact stress/penetration plots were generally similar to the contact stress diagrams themselves; this observation also generally agrees with the findings of reference 6. It seems therefore that simple methods based on

Winkler's hypothesis (10) are valid only in cases in which either (a) the footing is relatively stiff so that under all loading conditions contact stress distribution is nearly uniform (except at the edges) or (b) the loading is such that substantial variation of contact stress along the interface is not anticipated, the latter is difficult to determine and in fact is the crux of the problem.

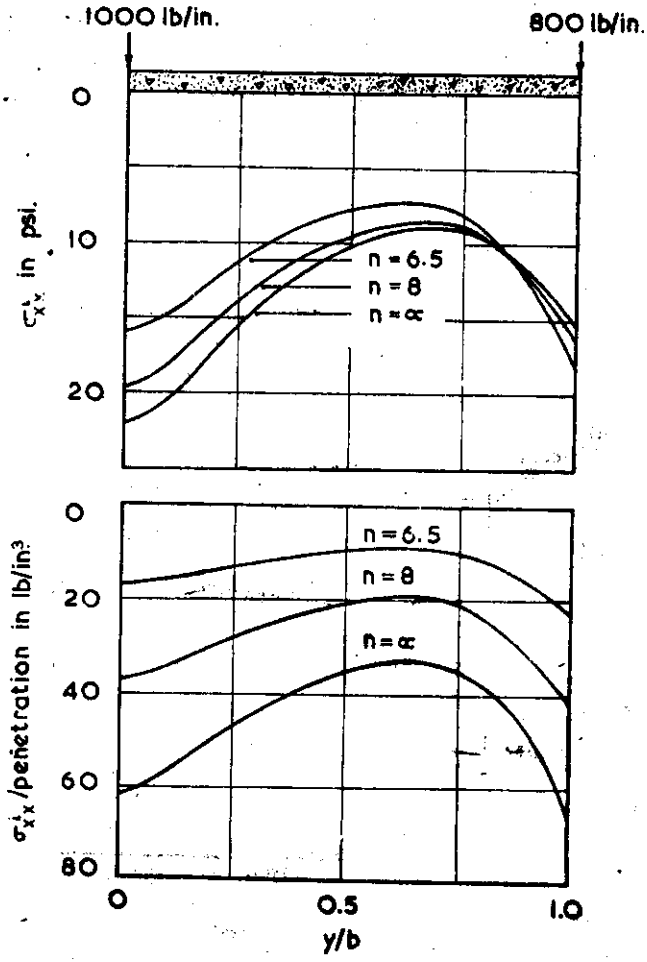

Fig. 12. **Response with multiple loads, d=0; ν=0.3; b=100 in.; G=2.00 psi.; ς=1.0**

4. The problem considered in this paper was rather simple in that non-linearities due to separation at the interface and material properties were assumed to be absent; further, the medium was assumed to terminate on a rigid strata at a finite depth, which is not usually the case. In a real situation, a combination of these complexities, among others, would exist. In addition, of course the harmonic responses would have to be integrated in the frequency domain to give responses of the system to a given arbitrary excitation. These aspects underline the complexities of the problem and frustrate, particularly in case of non-linear material properties, any attempt to produce a simple method for

its solution. At the moment a comprehensive program is in progress to solve the various aspects of this problem by using the finite element method; results of this study will be reported soon.

CONCLUSIONS

The following observations are made in conclusion.

1. For a given set of vertical harmonic loads and level of critical damping, the contact stress response depended mainly on the stiffness factor, q, defined as the ratio of stiffness of the soil medium to that of the footing. For a relatively flexible ($q>0\cdot1$) footing, the distribution of contact stress depended additionally on the way the loads were arranged on the footing, while, for stiff ($q<0\cdot1$) footings, the contact stresses were insensitive to the arrangement of loads; the stress distribution now resembled that due to the classical rigid block indenting into the medium, producing stress concentrations at the edges.

2. For a given set of parameters, the real part of stress response decreased with increasing frequency of motion, while, response at quadrature with loads increased.

3. Plots of contact stress/penetration ratios at the interface were generally similar to the contact stress plots themselves; thus, simpler methods of analysis based on Winkler's hypothesis (which assumes contact stress/penetration ratios to be constant along the interface) are valid, at least in systems involving strip footings, only for a limited category of flexible footing problems in which the ratio stress/penetration does not vary appreciably along the interface.

4. The coupled natural frequencies of the system were different from those of the footing and the soil medium separately. Present results show that coupling reduced the fundamental frequency of the soil medium by amounts which depended on the degree of coupling between the soil and the footing. With $q=0\cdot2$ for example, the reduction was found to be around 6%; however, this is an area of the problem in which much work remains to be done.

5. Finally, it is interesting to note that, although contact stresses decreased with increased exciting frequency in the sub-fundamental range considered, the penetration of the footing into the soil medium, nevertheless, increased and reached resonant proportions as the exciting frequency approached the fundamental natural frequency of the footing-soil system. To verify this, consider the problem of multiple loads in Figs. 7 and 8; with $q=0\cdot1$, the penetration of the footing at the origin ($x=0$, $y=0$) at various exciting frequencies, for example, can be computed from the data of figures 7 and 8 to give,

n	stress (psi)	stress/penetration (lb/in^3)	penetration (in)
∞	13·10	40·00	0·328
8·0	10·35	22·80	0·454
6·5	7·01	9·92	0·703

The last column shows clearly that penetration increased with increased frequency of motion.

ACKNOWLEDGEMENT

Thanks are due to the University of London computing Authorities for running the programs.

REFERENCES

1. Harr, M. E. et al, "Euler beam on a two parameter foundation model", Proc. ASCE, SM-4, Vol. 95, July 1969, pp. 933-948.
2. Zienkiewicz, O. C and Newton, R. E, "Coupled vibrations of a structure submerged in a compressible fluid", Proceedings, International Symposium on Finite Element Techniques, Stuttgart, May 1969.
3. Lysmer, J and Kuhlemeyer, R. L, "Finite Dynamic model for an infinite media", Journal of the Engineering Mechanics Division, ASCE, Vol. 95, EM-4, August 1969, pp. 859-877.
4. Cheung, Y. K and Zienkiewicz, O. C, "Plates and Tanks on Elastic Foundations—an application of finite element method", Int. J. solids and structures, Vol. 1, 1965, pp. 451-461.
5. Cheung, Y. K and Nag, D.K, "Plates and beams on Elastic foundations—Linear and non-linear behaviour", Geotechnique, Vol. 18, 1968, pp. 350-260.
6. Vesic, A.B and Johnson, W. H, "Model studies of beams resting on a silt subgrade", Proc. ASCE, SM-1, Feb. 1963, pp. 1-31.
7. Durelli, A. J et al. "Photoelastic study of beams on Elastic foundations", Proc. ASCE, ST-8, August 1969, pp. 1713-1725.
8. Filonenko-Borodich, M, "Theory of Elasticity", Dover Publications Inc., New York.
9. Awojabi, A. O, and Grootenhuis, P, "Vibration of rigid bodies on semi-infinite elastic media", Proceedings of the Royal society, A, Vol. 287, 1965, pp. 27-63.
10. Hetenyi, M, "Beams on Elastic foundation", The University of Michigan press, Ann Arbor, Michigan, 1946.

APPENDIX I

The values of e_{yy} on $x=0$, to be used in Eq. (2) can be found as follows :

If Eqs. (1) instead of Eq. (2) were used to solve the problem, then the displacements u(x, y, t) and v (x, y, t) must satisfy the conditions,

$$(\lambda+2G)\, u_{,x}+\lambda v_{,y}=0 \quad \text{and} \quad u_{,y}+v_{,x}=0$$

at the free surface; further, at the interface we must have,

$$u\,(0, y, t)=U(t)+\delta(y, t) \quad \text{and} \quad u_{,y}+v_{,x}=0$$

Other boundary conditions are the same as those described in text.

The various differential operators in Eq. (1) can now be replaced by their corresponding matrix operators, which satisfy the above boundary conditions. The resulting equation and Eq. (4) (with minor modification) constitute an alternative set of coupled equations, which can be solved to give the required values of e_{yy} on $x=0$.

The differential operators associated with Eq. (1) are,

$$\propto \frac{\partial^2}{\partial x^2}+\frac{\partial^2}{\partial y^2}\,,\ \frac{\partial^2}{\partial x^2}+\propto \frac{\partial^2}{\partial y^2} \quad \text{and} \quad \beta\,\frac{\partial^2}{\partial x \partial y}$$

These operators also appear in Eq. (2); consequently, the matrix operators of Eq. (1) can be taken from those of Eq. (2) and adjusted to comply with the conditions at $x=0$ discussed above. This reduces storage requirements and facilitates computation considerably.

APPENDIX II NOTATION

b	Half-width of the footing.
c	Velocity of shear waves in soil.
c′	Coefficient of viscous damping in soil.
d	Percent critical damping.
E	Young's modulus of the footing.
e_{xx}, e_{yy}, e_{xy}	Direct and shear strains in soil.
G	Modulus of rigidity of soil.

H	Depth of soil layer.
n	Period parameter ($=cT/b$).
P	Concentrated line load on the footing.
q	Relative stiffness factor ($=Gb^3/Et^3$).
T	Period of oscillation.
t	Thickness of the footing ; time.
U	Vertical indentation of the footing, assumed to be rigid, into the soil medium.
u, v	Components of displacement in soil.
X, Y	Components of body forces.
α	$(2-2\nu)/(1-2\nu)$.
β	$1/(1-2\nu)$
θ	$(e_{xx}+e_{yy})$.
V^2	Laplace's operator in two dimensions.
$\delta(y, t)$	Deflections of the footing.
ρ	Mass density of soil.
λ	Lame's Elastic constant.
σ_{xx}, σ_{yy}	Direct stresses.
σ^1_{xx}	Direct vertical stress at the interface.